Nondiffractive feature of $\gamma N \to \rho^{\pm} N$ with ρ-meson electromagnetic multipole moments

Byung-Geel Yu[a], Kook-Jin Kong[a]

[a]*Research Institute of Basic Science, Korea Aerospace University, Koyang, Gyeonggi 412-791, Korea*

arXiv:1604.03691v2 [nucl-th] 26 Jan 2017

Abstract

We investigate photoproduction of charged ρ off the nucleon using $\rho(770) + \pi(140)$ Regge pole exchanges by considering the ρ-meson electromagnetic multipole moments. The significance of the Ward identity at the $\gamma\rho\rho$ vertex is emphasized for current conservation in the process. Given π exchange with the well-known coupling constants for $\gamma\pi\rho$ and πNN, we analyze the role of the ρ exchange in the $\gamma p \to \rho^+ n$ and $\gamma n \to \rho^- p$ processes without model-dependences except for the magnetic moment $\mu_{\rho^\pm} = \pm 2.01$ and electric quadrupole moment $Q_{\rho^\pm} = \pm 0.027$ fm^2 taken from theoretical estimates. The nondiffractive feature of both cross sections is reproduced with a rapid decrease beyond the resonance region by the dominance of π exchange over the ρ. Cross sections for differential and density matrix elements are presented to compare with existing data. The parity and photon polarization asymmetries are predicted to demonstrate the apparent roles of the ρ-meson electromagnetic multipole moments.

Keywords: charged ρ meson, electromagnetic multipole moments, parity asymmetry, photoproduction, Regge model

A charged ρ-meson has electromagnetic (EM) multipole moments, where the canonical values for the magnetic dipole and electric quadrupole moments are expected to be $\mu_\rho = e_\rho/m_\rho$ and $Q_\rho = -e_\rho/m_\rho^2$ in the limit of a point-like particle [1]. Thus, it is interesting to investigate photoproduction of charged ρ [2],

$$\gamma + p \to \rho^+ + n, \tag{1}$$

$$\gamma + n \to \rho^- + p, \tag{2}$$

because they provide a testing ground for observing any deviations in the ρ-meson EM multipole moments from the canonical values due to the substructure of the vector meson.

Unlike much studied case of the ρ^0 process featuring diffractive Pomeron exchange [3], little is known about the production mechanism in the charged process.

In experimental studies, cross sections were measured for the total, differential, and spin density matrix elements of the $\gamma p \to \rho^+ n$ process in the energy range of $E_\gamma = 2.8 \sim 4.8$ GeV by the LAMP2 group [4], and at $E_\gamma = 9.6$ GeV by the Rochester-Cornell collaboration [5]. In the case of the $\gamma n \to \rho^- p$ process, the total and differential cross sections in the range $E_\gamma = 1{\sim}5$ GeV were extracted from the deuteron target by the ABBHHM collaboration at DESY [6, 7]. In particular, the data obtained from the latter process had a sharp peak in the cross section, with $\sigma_{max} \approx 7$ μb at around $E_\gamma \approx 1.6$ GeV and a steep decrease beyond the resonance region in a similar manner to the former process. Hence, both cross sections exhibit the typical features of a nondiffractive process, where photoproduction of the charged ρ is expected to proceed via nonresonant meson exchanges. We note that such a rapid decrease in the cross section over the peak with respect to the photon energy has also been observed in $\gamma p \to \rho^- \Delta^{++}$ [4] and $\gamma p \to K^* \Lambda$ photoproduction measured recently by the JLab CLAS collaboration [8].

In this work, we investigate charged processes $\gamma p \to \rho^+ n$ and $\gamma n \to \rho^- p$ within the Regge framework for $\rho + \pi$ exchanges, where we utilize the Born approximation amplitude for the gauge invariance of the t-channel ρ exchange. Existing data regarding the cross sections, including spin density matrix elements, are analyzed without fit parameters because we use no cutoff function for the Regge pole exchange. Moreover, the coupling constants related to the t-channel ρ and π exchanges are known from the decay width as well as another reaction process, i.e., pion photoproduction, so the role of ρ with the EM multipole moments can be clarified without model dependence.

However, previous studies of this issue were affected by the theoretical limits due to the difficulty establishing gauge invariance for the exchange of charged ρ with the $\gamma\rho\rho$ vertex coupling to charge, magnetic dipole, and electric quadrupole moments [2, 9, 10]. We recall that an on-shell vertex for the $\gamma\rho\rho$ coupling employed in these studies cannot satisfy the Ward identity, which should be addressed prior to any type of prescription for current conservation [11, 12]. In addition, a simplified charge-coupling of the $\gamma\rho\rho$ vertex was considered previously in the Regge model for the $\gamma N \to \rho^\pm N$ process [13]. By satisfying gauge invariance, the model obtained agreement with existing data.

As depicted in Fig. 1, the divergence of the $\gamma\rho\rho$ vertex should respect the Ward identity [11],

$$k_\mu \Gamma^{\mu\nu\alpha}_{\gamma\rho\rho}(q, Q) = (D^{-1})^{\nu\alpha}(q) - (D^{-1})^{\nu\alpha}(Q) \tag{3}$$

with respect to the propagator chosen in the unitary gauge,

$$D^{\nu\alpha}(q) = \frac{-g^{\nu\alpha} + q^\nu q^\alpha/m_\rho^2}{q^2 - m_\rho^2} \tag{4}$$

Email addresses: bgyu@kau.ac.kr (Byung-Geel Yu), kong@kau.ac.kr (Kook-Jin Kong)

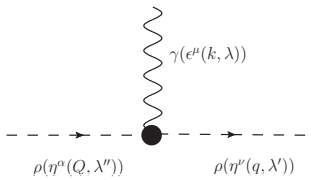

Figure 1: $\gamma\rho\rho$ vertex for the incoming and outgoing ρ of the momenta and polarizations $(Q\,,\lambda'')$ and $(q,\ \lambda')$.

and its inverse

$$(D^{\nu\alpha})^{-1}(q) = (q^2 - m_\rho^2)\left(g^{\nu\alpha} - \frac{q^\nu q^\alpha}{q^2}\right) - m_\rho^2\frac{q^\nu q^\alpha}{q^2}\,. \tag{5}$$

The identity in Eq. (3) allows us to derive the charge coupling term in the $\Gamma^{\mu\nu\alpha}_{\gamma\rho\rho}$ vertex, i.e.,

$$\begin{aligned} & e_\rho\eta^*_\nu\Gamma^{\mu\nu\alpha}_{\gamma\rho\rho}(q,Q;k)\eta_\alpha\epsilon_\mu \\ &= -\eta^*_\nu(q)e_\rho\Big\{[(q+Q)^\mu g^{\nu\alpha} - Q^\nu g^{\mu\alpha} - q^\alpha g^{\mu\nu}] \\ &\quad +\kappa_\rho(k^\nu g^{\mu\alpha} - k^\alpha g^{\mu\nu}) - \frac{(\lambda_\rho+\kappa_\rho)}{2m_\rho^2}\Big[(q+Q)^\mu k^\nu k^\alpha \\ &\quad -\frac{1}{2}(q+Q)\cdot k(k^\nu g^{\mu\alpha} + k^\alpha g^{\mu\nu})\Big]\Big\}\eta_\alpha(Q)\epsilon_\mu(k)\,, \end{aligned} \tag{6}$$

which leads to the conservation of current in a rather simple manner, which is similar to the case of pion photoproduction with the contact term. In this case, $\epsilon^\mu(k)$ and $\eta^\nu(q)$ are polarizations of the photon and ρ-meson for momenta k and q, respectively. The ρ-meson magnetic moment with the anomalous magnetic moment κ_ρ is taken from Lee and Yang [14], and the electric quadrupole moment λ_ρ is taken to be gauge-invariant itself according to Gross and Riska [12]. For on-shell $\gamma\rho\rho$ coupling, i.e., $\eta^*\cdot q = 0$, they are reduced to $\mu_\rho = (1+\kappa_\rho)\frac{e_\rho}{2m_\rho}$ and $\mathcal{Q}_\rho = \lambda_\rho\frac{e_\rho}{m_\rho^2}$ with $\kappa_\rho = 1$ and $\lambda_\rho = -1$ for a point-like ρ meson [1], as stated earlier. In this study, we select $\kappa_\rho = 1.01$ in favor of its naturalness and $\lambda_\rho = -0.41$ in accordance with $\mathcal{Q}_\rho = -0.027$ fm^2 [15].

We now consider the production amplitude for the $\gamma N \to \rho^\pm N$ process based on the diagrams shown in Fig. 2. Considering the parity and decay channels predicted in previous studies, the fully accounted amplitude will comprise the scalar meson $a_0(980)$, tensor meson $a_2(1320)$, and axial mesons $a_1(1260)$ and $b_1(1235)$, in addition to ρ and π exchanges in the t-channel. For simplicity and clarity, we consider the model of ρ+π exchanges, although the remainder have minor roles with contributions at an order of 10^{-2} at most according to the coupling constants predicted in Refs. [16, 17, 18], as well as based on the analysis of the Regge-pole fit to the data [19].

Then, in order to obtain a fair description of existing data up to $E_\gamma \simeq 10$ GeV, it is natural to employ G-parity counting to determine the phases of the degenerate trajectories ρ-a_2 and π-b_1 in a similar manner to pion photoproduction [20, 16]. To identify the sign of the photon-meson coupling, it is convenient to define the G-parity for a photon in the case where the isoscalar part of the photon is G-parity negative and the isovector part is G-parity positive [21]. In the diagrams of the t-channel exchanges shown in Fig.2, the G-parity negative π and G-parity

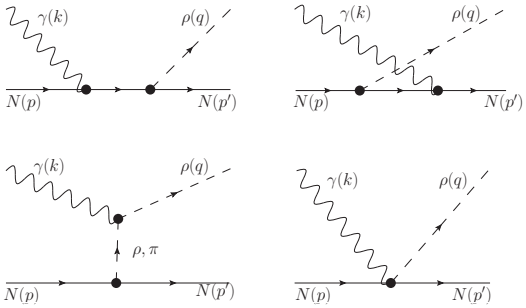

Figure 2: Feynman diagrams for $\gamma N \to \rho^\pm N$. Nucleon pole terms in the s- and u-channels are necessary together with the contact term for the gauge invariance of the t-channel ρ exchange.

positive ρ couple with the isoscalar photon, which does not change sign in the $\gamma\pi\rho^\pm$ vertex, whereas the G-parity positive b_1 and ρ couple to the isovector photon, which changes sign in the $\gamma b_1\rho^\pm$. Therefore, the signs of the exchange-degenerate (EXD) mesons in the production amplitudes can be written as

$$\begin{aligned} \mathcal{M}(\gamma N \to \rho^\pm N) &\propto (\pm\rho + a_2) + (\pi \pm b_1)\ , \\ &\propto \left\{\begin{array}{c} \rho\, e^{-i\pi\alpha_\rho(t)} + \pi e^{-i\pi\alpha_\pi(t)} \\ -\rho(-1) + \pi(1) \end{array}\right\} + \cdots\,, \end{aligned} \tag{7}$$

where the respective phases are determined according to the addition of each canonical phase, $\frac{1}{2}((-1)^J + e^{-i\pi\alpha_J(t)})$. The ρ exchange with signs denoting the ρ-meson charge e_ρ represents the gauge-invariant amplitude $\mathcal{M}_{\rho^\pm N}$, as given in Eqs. (12) and (13) in the following.

In numerical calculations, either the complex or constant phase for the ρ exchange will reproduce a slow decrease in the cross section according to the energy-dependence,

$$\sigma \propto s^{\alpha(0)-1}, \tag{8}$$

which contradicts the rapid slope in the decrease observed in both cross sections. Furthermore, the $\rho + \pi$ exchanges with the EXD phases in Eq. (7) are largely overestimated for both cross sections, unless the intercept of the ρ trajectory is smaller than usual, e.g., $\alpha_\rho(t) = 0.8\,t + 0.35$. Therefore, to obtain agreement with the experiments, we must use the cutoff function with the trajectory $\alpha_\rho(t) = 0.8\,t + 0.55$, as conventionally adopted by Laget [13], or we assume a violation of the EXD in one of these ρ-a_2 and π-b_1 pairs, as employed by Clark and Donnachie [19]. To favor the dominance of π exchange with the EXD phase over ρ, we break the EXD of the ρ-a_2 pair to assign the canonical phase, $\frac{1}{2}(-1 + e^{-i\pi\alpha_\rho})$ to ρ with the trajectories for ρ and π employed in previous studies [19, 22],

$$\alpha_\rho(t) = 0.9\,(t - m_\rho^2) + 1, \tag{9}$$

$$\alpha_\pi(t) = 0.7\,(t - m_\pi^2), \tag{10}$$

which are in better agreement with the total cross section data.

Given the Regge pole,

$$\mathcal{R}^\varphi(s,t) = \frac{\pi\alpha'_J}{\Gamma[\alpha_J(t)+1-J]\sin[\pi\alpha_J(t)]}\left(\frac{s}{s_0}\right)^{\alpha_J(t)-J}\ , \tag{11}$$

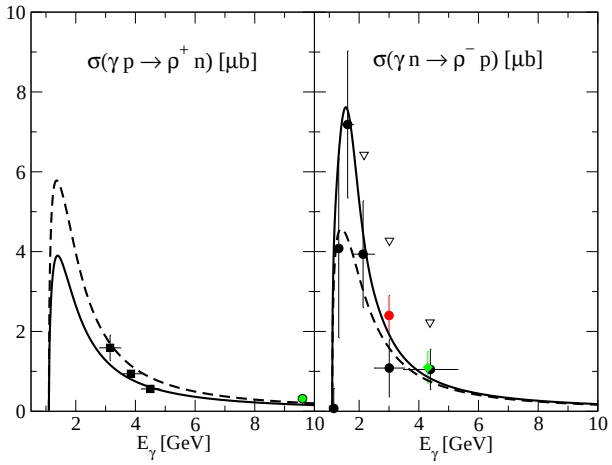

Figure 3: Dependence of the total cross section on the sign of the $\gamma\pi\rho$ coupling for ρ^+ (left) and ρ^- (right) processes. Solid lines represent results based on $g_{\gamma\pi\rho} = -0.224$ for π exchange plus the ρ exchange with $\kappa_\rho = 1.01$ and $\lambda_\rho = -0.41$. Dashed lines denote the case where $g_{\gamma\pi\rho} = +0.224$. The data are from previous studies [4, 5, 6, 7]

written collectively for a meson φ of spin-J, the conserved ρ-exchange for $\gamma p \to \rho^+ n$ is given by

$$\mathcal{M}_{\rho^+ n} = \sqrt{2}\,\bar{u}(p')\eta^*_\nu(q)\Big(\Gamma^\nu_{\rho pn}(q)\frac{\not{p}+\not{k}+M_p}{s-M_p^2}\Gamma^\mu_{\gamma pp}(k) + e\Gamma^{\mu\nu\alpha}_{\gamma\rho\rho}(q,Q)D_{\alpha\beta}(Q)\Gamma^\beta_{\rho pn}(Q) - e\frac{g^t_\rho}{4M_p}[\gamma^\nu,\gamma^\mu]\Big)\epsilon_\mu(k)u(p) \times (t-m_\rho^2)\times\mathcal{R}^\rho(s,t)\times\frac{1}{2}\left(-1+e^{-i\pi\alpha_\rho(t)}\right), \quad (12)$$

and for $\gamma n \to \rho^- p$,

$$\mathcal{M}_{\rho^- p} = \sqrt{2}\,\bar{u}(p')\eta^*_\nu(q)\Big(\Gamma^\mu_{\gamma pp}(k)\frac{\not{p}'-\not{k}+M_p}{u-M_p^2}\Gamma^\nu_{\rho pn}(q) - e\Gamma^{\mu\nu\alpha}_{\gamma\rho\rho}(q,Q)D_{\alpha\beta}(Q)\Gamma^\beta_{\rho np}(Q) + e\frac{g^t_\rho}{4M}[\gamma^\nu,\gamma^\mu]\Big)\epsilon_\mu(k)u(p) \times (t-m_\rho^2)\times\mathcal{R}^\rho(s,t)\times\frac{1}{2}\left(-1+e^{-i\pi\alpha_\rho(t)}\right), \quad (13)$$

respectively. The coupling vertices γNN and ρNN are given by

$$\Gamma^\nu_{\rho NN}(q) = g^v_\rho\gamma^\nu + \frac{g^t_\rho}{4M}[\gamma^\nu,\not{q}], \quad (14)$$

$$\Gamma^\mu_{\gamma pp}(k) = e\gamma^\mu - \frac{e\kappa_p}{4M}[\gamma^\mu,\not{k}], \quad (15)$$

where g^v_ρ=2.6 and g^t_ρ=9.62 are taken from the vector dominance with the ratio of $g^t_\rho/g^v_\rho = 3.7$, which is consistent with the nucleon's anomalous magnetic moment. For Reggeization, we introduce the nucleon pole term for the gauge invariance of the t-channel vector meson exchange. Given the significance of the magnetic interaction of the spin-1 particle, we preserve the nucleon magnetic moment $\kappa_p = 1.79$ in the s-channel for the $\gamma p \to \rho^+ n$ process, and in the u-channel proton pole term for $\gamma n \to \rho^- p$.

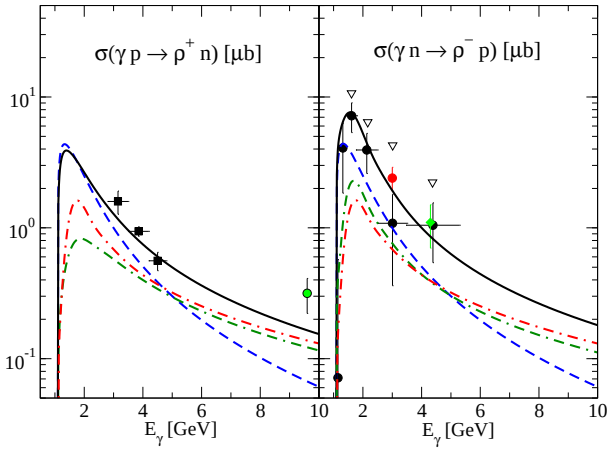

Figure 4: Contributions of ρ and π exchanges to the total cross section for ρ^+ and for ρ^- processes. The dashed line (blue) is due to π exchange and the dash-dotted line (red) is based on the single ρ exchange. The dash-dash-dotted line (green) is obtained from the gauge-invariant ρ exchange, $\mathcal{M}_{\rho^\pm N}$.

For the π exchange, we write the Regge-pole amplitude as

$$\mathcal{M}_{\pi^\pm} = i\sqrt{2}\,\frac{g_{\gamma\pi\rho}}{m_0}g_{\pi NN}\varepsilon^{\mu\nu\alpha\beta}\epsilon_\mu\eta^*_\nu k_\alpha q_\beta\,\bar{u}(p')\gamma_5\,u(p) \times\mathcal{R}^\pi(s,t)\times\left\{\begin{array}{c} e^{-i\pi\alpha_\pi(t)} \\ 1 \end{array}\right\}, \quad (16)$$

for $\gamma p \to \rho^+ n$ (upper), and $\gamma n \to \rho^- p$ (lower) with $g_{\pi NN} = 13.4$ and the mass parameter $m_0 = 1$ GeV. Then, the coupling constant $|g_{\gamma\pi\rho}| = 0.224$ is estimated from the width $\Gamma_{\rho^\pm\to\pi\gamma} = 68$ keV, and we take the sign of the π contribution with $\gamma\pi\rho$ coupling relative to ρ in order to achieve more consistency with existing data related to both processes.

Figure 3 shows the dependence of the total cross sections on the sign of the $g_{\gamma\pi\rho}$ coupling constant for the ρ^+ and for ρ^- processes. We recall that the charge asymmetry of the charged ρ photoproduction off the deuteron target was measured by Abramson et al. [5] as

$$\frac{\sigma_{\gamma d\to\rho^+ m} - \sigma_{\gamma d\to\rho^- m}}{\sigma_{\gamma d\to\rho^+ m} + \sigma_{\gamma d\to\rho^- m}} \approx -0.11 \pm 0.03, \quad (17)$$

based on the average of the invariant mass $M_{\pi^+\pi^-}$ interval. Thus, we can determine the ratio $\sigma_{\gamma d\to\rho^- m}/\sigma_{\gamma d\to\rho^+ m} \approx 1.25$ to predict that σ_{ρ^-} is larger than σ_{ρ^+} in Fig. 3. This is true for the ratio of the total cross sections between π^+ and π^- processes, which have the same isospin structure as ρ^+ and ρ^- processes. Thus, the $g_{\gamma\pi\rho}$ positive case is discarded.

Figure 4 shows the contributions of ρ and π exchanges. The dominance of the latter exchange before $E_\gamma \simeq 5$ GeV in both processes is responsible for the steep decrease in both cross sections. As shown in the figure, the different contributions of $|\rho-\pi|^2$ (ρ denotes $\mathcal{M}_{\rho^\pm N}$ on the green line) for ρ^+ and $|-\rho-\pi|^2$ in ρ^- production via the negative coupling $\gamma\pi\rho$ can help us to understand the relative size of the cross sections in this region. Above $E_\gamma \simeq 5$ GeV, the contribution of ρ exchange dominates that of π, as shown by the experimental data obtained at $E_\gamma = 9.6$ GeV [5].

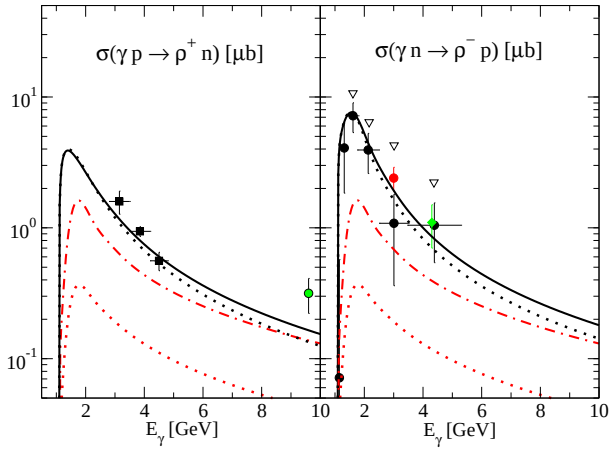

Figure 5: Dependence of the total cross section on the EM multipole mome of the ρ-meson. The red dotted line is based on the single ρ exchange w $\kappa_\rho = 0$ and $\lambda_\rho = 0$. The black dotted line is the resulting σ obtained for the process (left), and similarly for the ρ^- process (right).

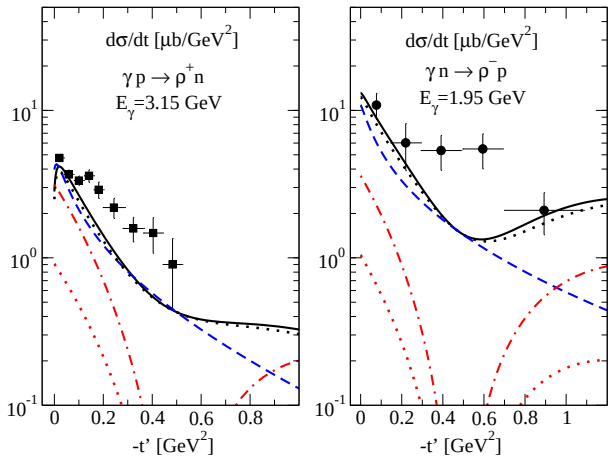

Figure 6: Contributions of π and ρ exchanges to the differential cross section for ρ^+ at $E_\gamma = 3.15$ GeV and for ρ^- at $E_\gamma = 1.95$ GeV. The notations are the same as those used in Figs. 4 and 5. The data are from previous studies [4, 7].

The roles of the EM multipole moments of ρ exchange are illustrated in Fig. 5 in order to show the contributions of κ_ρ and λ_ρ to the cross section. The single ρ exchange (the t-channel exchange in Fig. 2) with and without these contributions differs by an order of magnitude, as shown by the dash-dotted and dotted lines. The role of κ_ρ is more significant than that of λ_ρ.

The differential cross sections for ρ^+ and ρ^- processes are presented in Fig. 6, which exhibit a dipped structure for ρ exchange at $-t \approx 0.5$ GeV$^2/c^2$ due to the nonsense-wrong-signature-zero of the ρ trajectory, i.e., $\alpha_\rho(t) = 0$, from the canonical phase. This feature makes the angular distribution increasing over $-t \approx 0.5$ GeV$^2/c^2$, which is apparent in the differential cross sections of ρ^+ in other energy ranges, as shown in Fig. 7. However, we need more data to confirm such a structure for the ρ^- process. We note that our estimate of the contribution of the π exchange to $d\sigma/dt$ at $E_\gamma = 9.6$ GeV in the ρ^+ process is

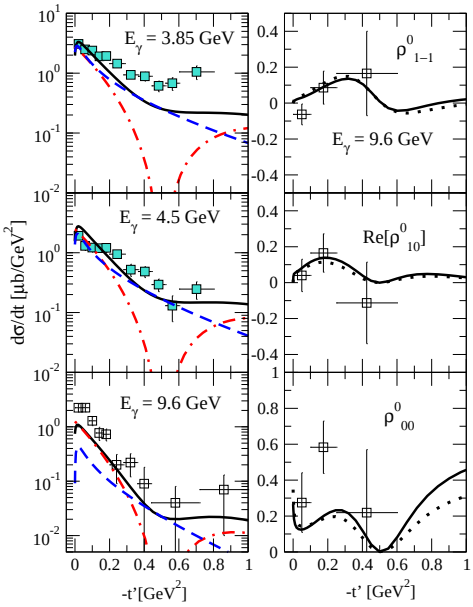

Figure 7: Differential cross sections in three energy bins and density matrix elements $\rho^0_{\lambda\lambda'}$ at $E_\gamma = 9.6$ GeV for $\gamma p \to \rho^+ n$. The notations are the same as those used in Fig. 6. Data for the full-square are from Barber et al. [4] and those for the empty-square are from Abramson et al. [5].

similar to that given by Abramson et al. [5], but different from that provided by Benz et al. [7] at $E_\gamma = 1.95$ GeV in the ρ^- process.

Figure 7 shows the differential cross sections together with the density matrix elements $\rho^0_{\lambda\lambda'}$ estimated in the Gottfried-Jackson frame [23, 24] for the unpolarized ρ^+ process. Since the latter observables relate the spin polarization of the final vector meson to that of the initial photon in the helicity amplitude, the spin correlations involved in the production mechanism provide a further test of the validity of the model predictions. In our proposed framework, the density matrix elements are reproduced by the oscillatory behavior of the ρ exchange due to the canonical phase and thus they agree with the data.

Finally, we present model predictions for the parity asymmetry [23] $P_\sigma = 2\rho^1_{1-1} - \rho^1_{00}$ at $\theta = 1^\circ$ in the c.m. frame and the photon polarization asymmetry [24] $\Sigma = 2\rho^1_{11} + \rho^1_{00}$ at $\theta = 30^\circ$ in Fig. 8. The role of the ρ-meson EM multipole moments is apparent in these observables, so the measurements of P_σ and Σ could be useful for guiding the determination of μ_ρ and λ_ρ in experiments.

In summary, we investigated photoproduction of charged ρ for positive and negative cases based on the Regge model, where the $\gamma\rho\rho$ vertex fully accounted for the magnetic dipole and electric quadrupole moments. We stressed the validity of the Ward identity of the $\gamma\rho\rho$ vertex for the gauge invariance of the process. Using the non-degenerate phase for the ρ exchange based on empirical evidence for a steep decrease in the cross sections, we showed that these processes are dominated by π exchange over ρ, thereby demonstrating the nondiffractive feature of the processes, as well as the dipped structure in the differential cross section and the oscillatory behavior of the density matrix. We investigated the role of the ρ-meson

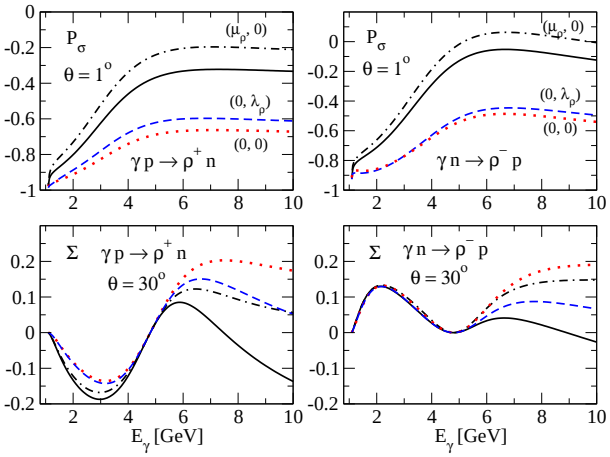

Figure 8: Energy dependence of the parity asymmetry P_σ and photon polarization asymmetry Σ. The labels on the curves denote whether the EM multipole moments are turned on and off.

EM multipole moments $\mu_{\rho^\pm} = \pm 2.01$ and $Q_{\rho^\pm} = \pm 0.027$ fm^2 to analyze the production mechanism based on comparisons with existing data. We predicted the parity and photon polarization asymmetries within the present framework to facilitate future experimental observations. In particular, measurements of cross sections for the $\gamma p \to \rho^+ n$ and $\gamma n \to \rho^- p$ processes in the resonance region are desirable to allow further development of the theory of photoproduction of charged vector meson.

Acknowledgments

We are grateful to Ho-Meoyng Choi for fruitful discussions. This work was supported by the grant NRF-2013R1A1A2010504 from the National Research Foundation (NRF) of Korea.

References

[1] S. Brodsky and J. R. Hiller, Phys. Rev. D **46**, 2141 (1992).
[2] R. D. Clark, Phys. Rev. **187**, 1993 (1969).
[3] J.-M. Laget, Nucl. Phys. A **699**, 184 (2002).
[4] D. P. Barber *et al.*, Z. Phys. C **2**, 1 1979.
[5] J. Abramson *et al.*, Phys. Rev. Lett. **36**, 1432 (1976).
[6] H. G. Hilpert *et al.*, Nucl. Phys. B **70**, 93 (1970).
[7] P. Benz *et al.*, Nucl. Phys. B **79**, 10 (1974).
[8] W. Tang *et al*, Phys. Rev. C **87**, 065204 (2013).
[9] H. Joos and G. Kramer, Z. Phys. **178**, 542 (1964).
[10] E. Tomasi-Gustafsson and M. P. Rekalo, Eur. Phys. J. A. **21**, 469, (2004).
[11] U. Baur and D. Zeppenfeld, Phys. Rev. Lett. **75**, 1002 (1995)
[12] F. Gross and D. O. Riska, Phys. Rev. C **36**, 1928 (1987).
[13] J. M. Laget, Phys. Lett. B **695**, 199 (2011).
[14] T. D. Lee and C. N. Yang, Phys. Rev. **128**, 885 (1962).
[15] M. S. Bhagwat and P. Maris, Phys. Rev. C **77**, 025203 (2008).
[16] B. G. Yu, T. K. Choi, and W. Kim, Phys. Rev. C **83**, 025208 (2011).
[17] S. Ishida, K. Yamada, and M. Oda, Phys. Rev. D **40**, 1497 (1989).
[18] G. Erkol, R. G. E. Timmermans, M. Oka, and T. A. Rijken, Phys. Rev. C **73**, 044009 (2006).
[19] M. Clark and A. Donnachie, Nuclear Materials B **125**, 493 (1977).
[20] M. Guidal, J.-M. Laget, and M. Vanderhaeghen, Nucl. Phys. A **627**, 645 (1997).
[21] H. J. Lipkin, *Lie Groups for Pedestrians*, North-Holland, 1965, p147.
[22] R. B. Clark, Phys. Rev. D **18**, 1444 (1978).
[23] K. Schilling, P. Seyboth, and G. Wolf, Nucl. Phys. B **15**, 397 (1970).
[24] Q. Zhao, J. S. Al-Khalili, and P. L. Cole, Phys. Rev. C **71**, 054004 (2005).